

Article

Temporal Variation and Spatial Distribution of Groundwater Level Changes Induced by Large Earthquakes

Ching-Yi Liu ¹, Yeeping Chia ², Po-Yu Chung ¹, Tsai-Ping Lee ³ and Yung-Chia Chiu ^{4,*}

¹ Advanced Geological Research Task Force, Sinotech Engineering Consultants, Inc., No. 280, Xinhua 2nd Rd., Neihu Dist., Taipei City 114, Taiwan

² Department of Geosciences, National Taiwan University, No. 1, Sec. 4, Roosevelt Rd., Taipei City 106, Taiwan

³ Taiwan Power Company, No. 242, Sec. 3, Roosevelt Rd., Zhongzheng District, Taipei City 100, Taiwan

⁴ Institute of Earth Sciences, National Taiwan Ocean University, No. 2, Beining Rd., Zhongzheng District, Keelung City 202, Taiwan

* Correspondence: ycchiu@mail.ntou.edu.tw; Tel.: +886-2-2462-2192 (ext. 6515)

Abstract: Sustained coseismic changes in groundwater level due to static strain during earthquakes could be considered as an indicator of crustal deformation. These changes usually occur abruptly but recover slowly after earthquakes. High-frequency data indicate a time lag between the coseismic change of well water levels and that of the groundwater levels in the aquifer. Abnormal post-seismic changes in groundwater level were observed, possibly caused by cross-formation flow, fracturing, or strain relief. Although sustained changes are generally induced by a local earthquake, they could also be triggered by a distant large earthquake that has occurred at the same tectonic plate. The magnitude and polarity of coseismic changes may vary in wells of different depths at multiple-well stations, revealing additional information about the complexity of crustal deformation in the subsurface. Coseismic falls dominated near the ruptured seismogenic fault during the 1999 M7.6 earthquake, which implied crustal extension adjacent to the thrust fault. However, coseismic rises prevail in most areas, suggesting that crustal compression caused by plate convergence plays a major role on the island of Taiwan during earthquakes.

Keywords: coseismic; groundwater; earthquake; deformation; sustained changes; post-seismic; high-frequency monitoring



Citation: Liu, C.-Y.; Chia, Y.; Chung, P.-Y.; Lee, T.-P.; Chiu, Y.-C. Temporal Variation and Spatial Distribution of Groundwater Level Changes Induced by Large Earthquakes. *Water* **2023**, *15*, 357. <https://doi.org/10.3390/w15020357>

Academic Editors: Costanza Cambi and Daniela Valigi

Received: 1 December 2022

Revised: 28 December 2022

Accepted: 13 January 2023

Published: 15 January 2023



Copyright: © 2023 by the authors. Licensee MDPI, Basel, Switzerland. This article is an open access article distributed under the terms and conditions of the Creative Commons Attribution (CC BY) license (<https://creativecommons.org/licenses/by/4.0/>).

1. Introduction

Changes in groundwater level due to large earthquakes have been documented for decades [1–4]. Sustained changes that have occurred abruptly during earthquakes have been attributed to the static strain caused by fault slip [5–7]. Oscillatory changes are the response of water pressure in the well and in the aquifer to the dynamic strain associated with passing seismic waves [1,8–10]. Generally, sustained changes are anticipated to be induced primarily by local earthquakes, while oscillatory changes can be triggered by local earthquakes as well as large, distant earthquakes [1,8,11–14].

The sustained change in groundwater level is usually recorded in a well, and thus, it is different from that in the connected aquifer. Large sustained changes are known to cause abnormal phenomena in hydrological and related processes after earthquakes, such as changes in streamflow [15,16], spring flow [17,18], water temperature [19,20], and chemical composition [21,22]. Even though plenty of studies have been reported, the detailed processes of sustained coseismic changes as well as post-seismic changes in the subsurface are not well understood.

The poroelastic theory [23,24], which involves coupling the fluid flow and soil deformation, has been proposed to explain the mechanism of sustained coseismic changes in groundwater level [23,25–27]. Therefore, sustained changes could be considered as indicators of crustal deformation. Moreover, the spatial distribution of coseismic changes

has the potential to reveal subsurface compression and extension [28,29]. Nevertheless, such studies are often hampered by scattered monitoring wells and limited data.

In this study, we present observations of coseismic and post-seismic changes in groundwater level induced by large earthquakes. The water level data, including high-frequency data, were recorded by a dense network of multiple-well monitoring stations in Taiwan. The associated temporal variations and spatial distributions of coseismic changes were examined. The insights and impacts of coseismic and post-seismic changes are discussed.

2. Materials and Methods

2.1. Monitoring Wells and Water Level Data

The island of Taiwan is located at the boundary between the Eurasian plate and the Philippine Sea plate. In southeastern Taiwan, the Philippine Sea plate moves northwestward and overrides the Eurasian plate with a convergent rate of approximately 80 mm per year. In northeastern Taiwan, however, the Philippine Sea plate moves northward and subducts beneath the Eurasian plate [30]. As part of the circum-Pacific seismic belt and the Pacific Ring of Fire, strong earthquakes occur frequently in Taiwan and its vicinity.

As a result of plate convergence, erosion, and deposition, Taiwan comprises mountain ranges running along the north–south direction in the east and coastal plains in the west. Figure 1 shows the distribution of monitoring well stations on the island. Nine hundred and seventy-five groundwater monitoring wells have been installed at 470 stations since 1992 for better management of groundwater resources. Among the installed wells, 807 are active and range in depth from 14 to 300 m. Hydrogeological investigations have been conducted for each station, providing comprehensive subsurface information prior to the placement of monitoring wells.

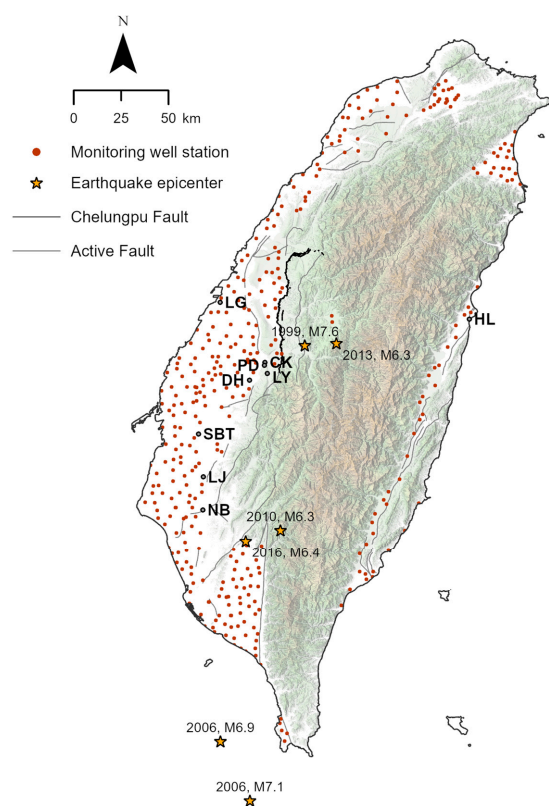


Figure 1. Map showing the epicenters of earthquakes and the locations of monitoring stations. The yellow stars represent the epicenters of the large, local earthquakes discussed in this study, and the dark-red circles represent monitoring stations in Taiwan. The characters show the locations of the nine monitoring wells used in this study.

The locations of monitoring well stations and the epicenters of the large, local earthquakes used in this study are marked in Figure 1. Each station is composed of one to five wells screened at different depths. The lithology for each station used in this study and the associated screen intervals are shown in Figure 2 (the lithology at Station CK was unreliable and not shown in the figure). The number following the station name (for example, LG1, LG2, and LG3) represents the relative screen depth of the well, i.e., the smaller and larger numbers imply the screen intervals located at shallower and deeper depths, respectively. The detailed screen depths, recording interval, aquifer lithology, and confining condition of each used well are listed in Table 1. Most of the wells are screened in sand or gravel aquifers. The distant earthquakes selected for discussion in this study are the M8.1 Wenchuan earthquake that occurred in central China on 12 May 2008 and the M9.0 Tohoku-oki Earthquake that occurred of the shore of east Japan on 11 March 2011.

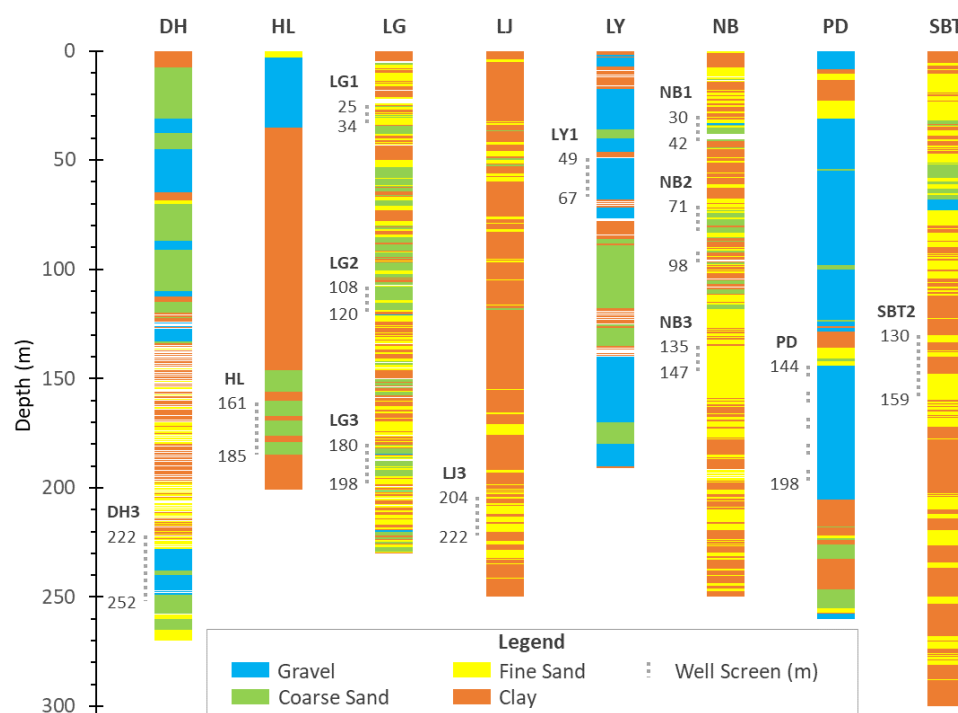


Figure 2. The associated hydrogeological units and screen intervals of the monitoring stations/wells used in the study. Each station might have multiple wells perforated at different depths (the lithology at Station CK was unreliable and not shown in the figure).

Table 1. Information on the monitoring wells used in this study.

Well Name	Screen Depth (m)	Recording Interval	Aquifer Lithology	Confining Condition
CK1	35–53, 71–89	1 h	Gravel	Confined
DH3	222–252	1 Hz	Gravel, and coarse sand	Confined
HL	161–185	1 Hz	Coarse sand	Confined
LG1	25–34	1 h	Coarse sand and fine sand	Confined
LG2	108–120	1 h	Coarse sand	Confined
LG3	180–198	1 h	Coarse sand and fine sand	Confined
LJ3	204–222	1 Hz	Fine sand and clay	Confined
LY1	49–67	1 h	Gravel	Confined
NB1	30–42	1 h	Coarse sand and fine sand	Confined
NB2	71–83, 92–98	1 h	Coarse sand and clay	Confined
NB3	135–147	1 Hz and 1 h	Fine sand	Confined
PD	144–150, 156–162, 168–174, 180–186, 192–198	1 h	Gravel	Confined
SBT2	130–159	2 min	Fine sand and clay	Confined

Well water levels were recorded every hour by the automated recording system at the monitoring well station. Recently, the monitoring interval has been improved to every 10 min. In addition, a high-frequency monitoring system was installed in a few wells to record the water level every second or every two minutes. These high-frequency data allow us to observe the detailed process of oscillatory changes and sustained changes triggered by earthquakes. The clocks in the sensors were synchronized to the GPS time (1-Hz data), and the Internet time server (2 min and 1 h data). Here, we used the local time (UTC+8) of earthquake occurrence.

Due to the gradual increase in installed monitoring wells since 1992, the number of wells used to analyze the coseismic changes in water levels has varied with earthquakes and their associated numbers should be dependent on the year that the earthquakes occurred. For the analysis of each earthquake, we used all of the active wells and the available data from when the event occurred.

2.2. Sustained Coseismic Changes

Both oscillatory and sustained coseismic changes in well water levels triggered by earthquakes have been recorded in the monitoring wells. Oscillatory changes are the response of water pressure in the well and in the aquifer to the dynamic strain associated with passing seismic waves [1,8–10]. Sustained changes caused by static strain due to fault slip have been considered as an indicator of crustal deformation during earthquakes [27,31,32]. Generally, a sustained rise in groundwater level implies a compressive strain while a fall implies an extensive strain. Moreover, the coseismic crustal strains may have a significant impact on the post-seismic subsurface and surface water flow [15,33]. Therefore, sustained changes become the focus of our study on coseismic changes in groundwater level.

Previous studies concerning the occurrence of sustained coseismic changes usually consider a time window within a few hours [5,11,34,35]. Sometimes this window extends to dozens of days [12]. With the improvement of monitoring technologies, nowadays it is possible to monitor water levels at the frequency of 1 Hz. Thus, the process of groundwater level change can be clearly observed. Here, the sustained coseismic change focus in this study is stated as the largest cumulative change in well water level that occurs within a few minutes to a few hours after the earthquake.

3. Results

3.1. Temporal Variation of Coseismic Changes in Groundwater Level

3.1.1. Processes of Sustained Coseismic Changes

Oscillatory changes in groundwater level can be observed in monitoring wells during large earthquakes by using high-frequency data. Figure 3a shows the occurrence of water-level oscillations induced by the 2010 M6.3 local earthquakes at well HL, where the water level was recorded once per second (1 Hz). The well water level continuously oscillated for 2.6 min after the arrival of seismic waves. The amplitude of oscillatory changes reflects the amplification of pore pressure oscillations in the aquifer [8]. The oscillations diminished shortly after seismic waves passed through, and then the water level returned to the pre-earthquake level.

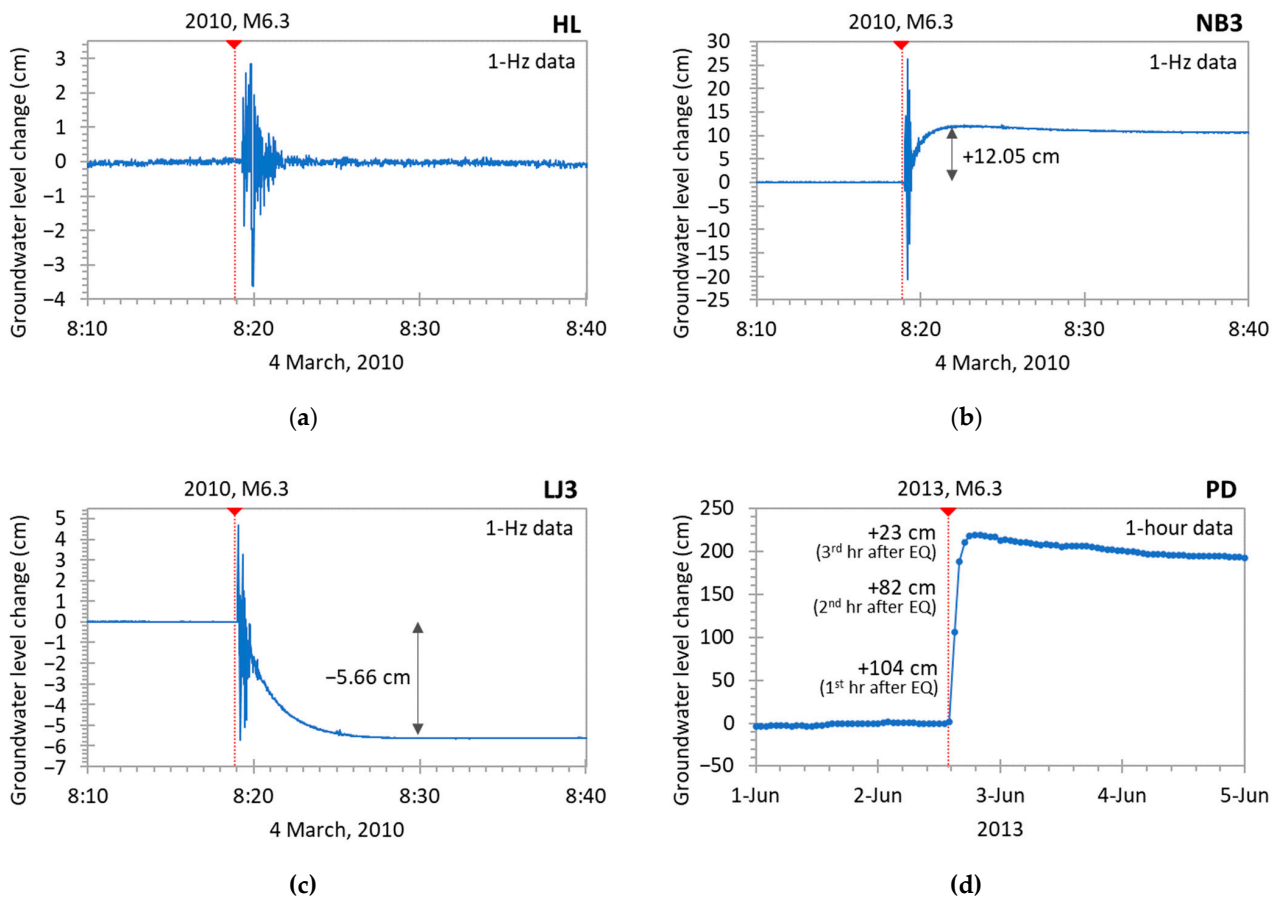


Figure 3. The process of coseismic changes in well water levels: (a) Oscillatory coseismic changes at the HL well, 1 Hz data, triggered by the 2010 M6.3 earthquake; (b) sustained coseismic rise at the NB3 well, 1 Hz data, triggered by the 2010 M6.3 earthquake; (c) sustained coseismic fall at the LJ3 well, 1 Hz data, triggered by the 2010 M6.3 earthquake; (d) delayed sustained coseismic rise at the PD well triggered by the 2013 M6.3 earthquake.

At some wells, sustained changes which alter the variation trend of the groundwater level were observed during oscillatory changes. Based on the theory of poroelasticity [23], these changes are considered to be caused by the static strain due to fault slip along the seismogenic fault during earthquakes [5,34]. Conceptually, the change in pore pressure is determined by both the groundwater flow and the change in the stress–strain state. At the moment of the earthquake, the pore pressure change in the confined aquifer caused by groundwater flow is very small. Therefore, coseismic change in pore pressure could be controlled primarily by the sudden change in stress–strain due to fault slip.

Based on 1 Hz data, Figure 3b shows a sustained rise of 12.05 cm in water level at well NB3 during the 2010 M6.3 earthquake. The process of the coseismic rise started during oscillatory changes and lasted for approximately 4 min. Figure 3c shows a sustained fall in the well water level during the earthquake at well LJ3. The process of the coseismic fall also occurred during oscillatory changes, lasting for about 13 min. The largest water level fall was 5.66 cm.

The sustained coseismic change in the groundwater level in the aquifer is expected to occur abruptly in response to a sudden stress redistribution. Nevertheless, the sustained change of well water level, based on 1 Hz data, shows a gradual process. In fact, the response time of the water level in the well is slower than that of the groundwater level in the aquifer. The delayed change in well water level is likely caused by groundwater flow driven by the coseismic change in the aquifer. The process continues until the water pressure in the well is in balance with that in the aquifer.

As most monitoring wells are screened in permeable aquifers, the water pressure often reaches a balance in a few to tens of minutes. However, at the PD well which was installed in a relatively less permeable aquifer, the largest sustained rise of 209 cm in well water level was reached 3 h after the 2013 M6.3 earthquake (Figure 3d).

3.1.2. Coseismic Changes Caused by Distant Earthquakes

Large distant earthquakes often trigger oscillatory changes in water level. Figure 4a shows water level oscillations at well DH3 for over 20 min following the arrival of seismic waves generated by the M9.0 Tohoku-oki Earthquake off the shore of east Japan on 11 March 2011. The peak amplitude is from 14.48 cm to -12.24 cm. The distance between the earthquake epicenter and the DH3 well is approximately 2600 km. When the oscillations ceased, the well water level returned to the pre-earthquake level. In fact, no sustained changes were recorded at 610 monitoring wells at 298 stations active in Taiwan following the earthquake.

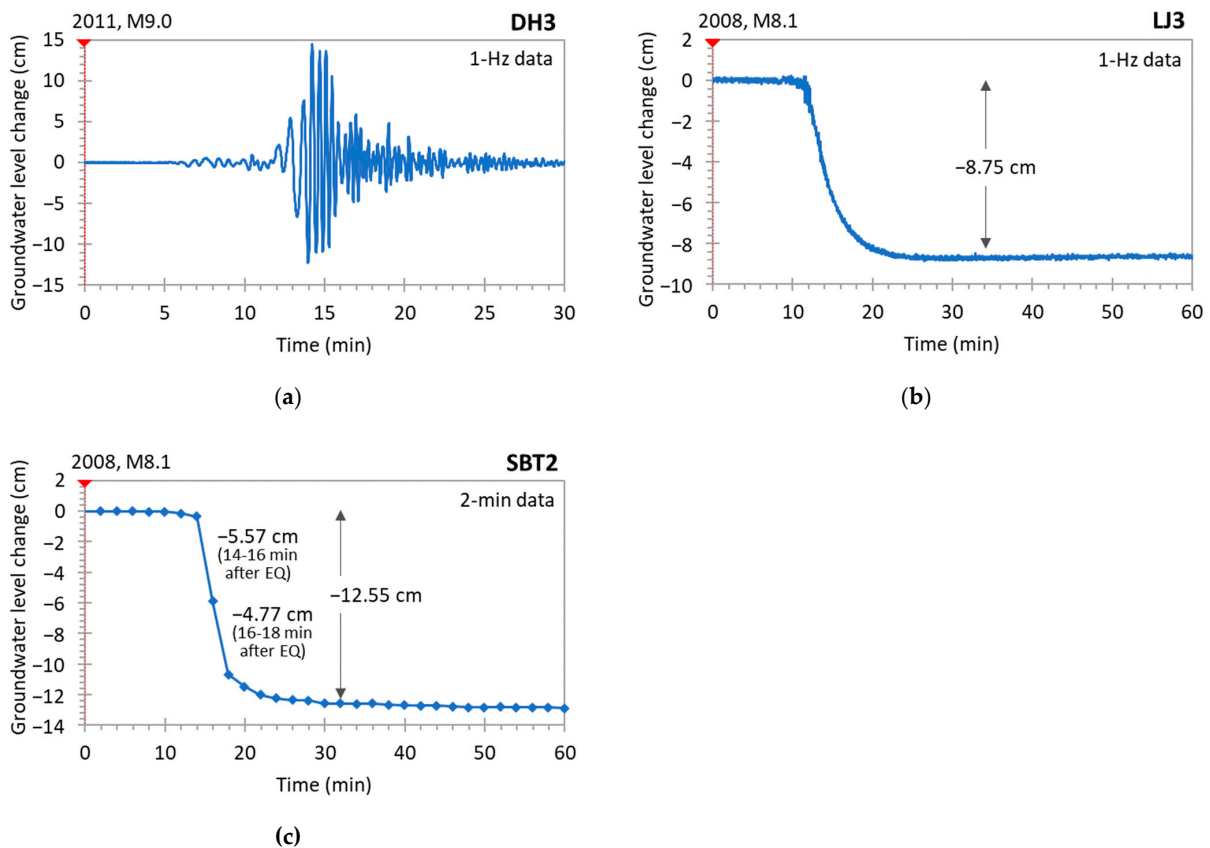


Figure 4. Changes in groundwater level due to large, distant earthquakes: (a) oscillatory changes in well DH3, recorded in 1 Hz frequency, following the 2011 M9.0 Tohoku-oki earthquake of the shore of east Japan; (b) sustained changes in well LJ3, recorded in 1 Hz frequency, following the 2008 M8.1 Wenchuan earthquake; (c) sustained changes in well SBT3, recorded every 2 min, following the 2008 M8.1 Wenchuan earthquake.

However, it is noted that sustained changes were recorded at several wells in Taiwan due to the large distant M8.1 Wenchuan earthquake that occurred in central China on 12 May 2008. Figure 4b,c show sustained coseismic changes at two wells of LJ3 and SBT2 in Taiwan. The distance from the earthquake epicenter to these two wells is about 1900 km. After the arrival of surface waves, based on the 1 Hz data, the water level at well LJ3 started to oscillate for 2 min, then declined gradually during the next 12 min until it reached a steady level approximately 8.75 cm below the pre-earthquake level (Figure 4b).

Based on the data recorded every two minutes, as shown in Figure 4c, the water level at well SBT2 changed slowly and slightly prior to the earthquake but fell 10.34 cm abruptly in 4 min starting from the 14th minute after the earthquake on May 12. The coseismic change took 22 min to complete the 12.55 cm fall. In fact, during the 2008 M8.1 Wenchuan earthquake, sustained changes in water level, ranging from -40 to $+23$ cm, were recorded at 80 monitoring wells in Taiwan [13]. The widespread changes suggested that the stress state in Taiwan could be changed by a distant, large earthquake.

3.1.3. Post-Seismic Changes in Groundwater Level

Since crustal deformation due to fault slip is ceased immediately after earthquakes, the pore pressure in the aquifer can no longer be changed by the stress–strain. Instead, groundwater flow starts to play a major role in determining post-seismic changes in pore pressure. As coseismic changes in pore pressure would drive groundwater flow to or from the adjacent formations after the earthquake, pore pressures are expected to recover gradually and steadily. Such a post-seismic recharge–discharge process may not only modify the groundwater flow system but affect the surface water flow system including stream flow and spring flow [15,17,18,31].

The post-seismic recovery of coseismic rises or falls of pore pressure due to groundwater flow in confined aquifers is a slow process, and thus, coseismic changes often sustain for a long period of time. Figure 5a shows the recovery process of a coseismic fall of 405 cm at well CK1 during the 1999 M7.6 earthquake. Well CK1 is 59 m deep, tapping a semi-consolidated rock aquifer. Apparently, the post-seismic recovery of the coseismic fall is rather slow. The water level recovered only about 30% ten days after the earthquake and returned to the pre-earthquake level 36 months after the earthquake's occurrence.

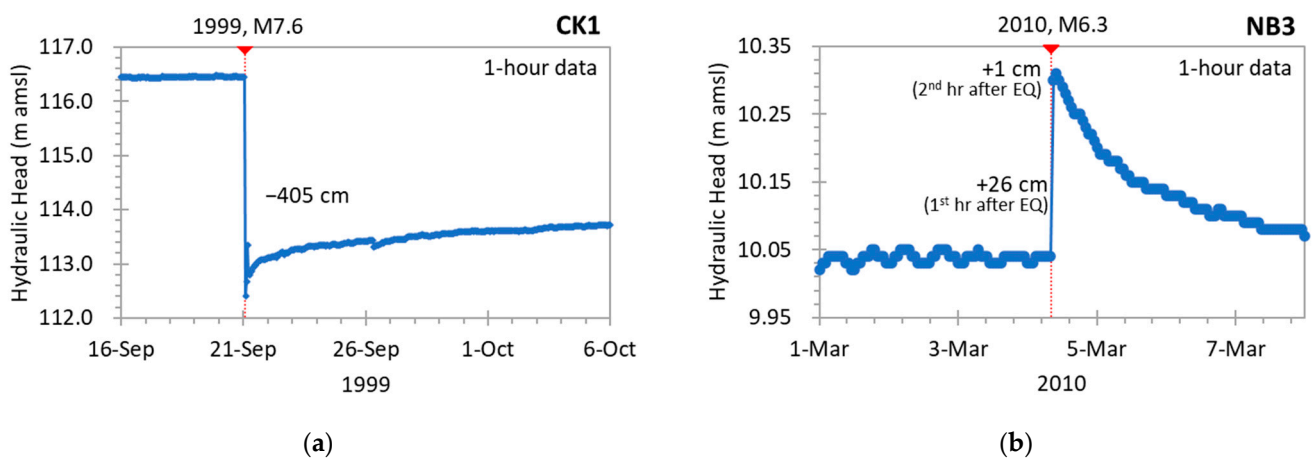


Figure 5. Post-seismic changes in well water level recorded in one hour frequency (the hydraulic head is plotted as the elevation above the mean sea level (m amsl)): (a) recovery of a coseismic fall in well CK1 after the 1999 M7.6 earthquake; (b) recovery of a coseismic rise in well NB3 after the 2010 M6.3 earthquake.

Figure 5b shows a relatively fast recovery process of a coseismic rise of 26 cm at well NB3 due to the 2010 M6.3 earthquake. The depth of well NB3 is 153 m. It is noted that the water level continued to rise 1 cm one hour after the earthquake, instead of a decline. Such a delayed rise in the well water level was likely caused by the post-seismic groundwater flow from the aquifer to the well. Starting from the second hour, the water level declined 1 cm every 1 to 6 h due to outflow of groundwater flow in response to the coseismic rise. The recovery rate was about 20% eight hours after the earthquake and recovered 85% three days after the event.

Abnormal recovery patterns after coseismic changes in groundwater level were observed occasionally. Previous studies [13,34] have indicated that cross-formational ground-

water flow may cause abnormal post-seismic recovery processes after coseismic changes. Moreover, rapid recovery processes immediately after earthquakes were observed. For instance, Figure 6a shows a coseismic fall of 72 cm at well NB3 followed by an anomalously rapid rise immediately after the 2016 M6.4 earthquake. The recovery rate of coseismic change was 33% in one hour, 57% in 2 h, and 69% in 4 h after the earthquake. After 4 h, the recovery began to slow down, similar to that after the 2010 M6.3 earthquake (Figure 4b). The contrast between Figures 5b and 6a suggests that the rapid rise during the first 4 h after the 2016 M6.4 earthquake was caused by an abnormal stress–strain-related process, instead of a hydrological process. In a few cases, recovery after a coseismic fall was not even observed. Figure 6b shows the post-seismic water level change of a coseismic fall of 658 cm in well LY1, tapping into a confined aquifer, during the 1999 M7.6 earthquake. It is noted that instead of a gradual rise after the earthquake, the water level declined continuously until the end of 1999. LY1 was originally an artesian well located near a river-bank, approximately 4.8 km from the seismogenic fault. After the coseismic fall, however, the well did not flow naturally any longer. Field investigations indicated that the nearby riverbank was ruptured during the earthquake. The fractures might provide permeable pathways for groundwater discharge from the artesian aquifer to the adjacent river [36,37]. Consequently, the water level in LY1 could no longer return to the pre-earthquake level.

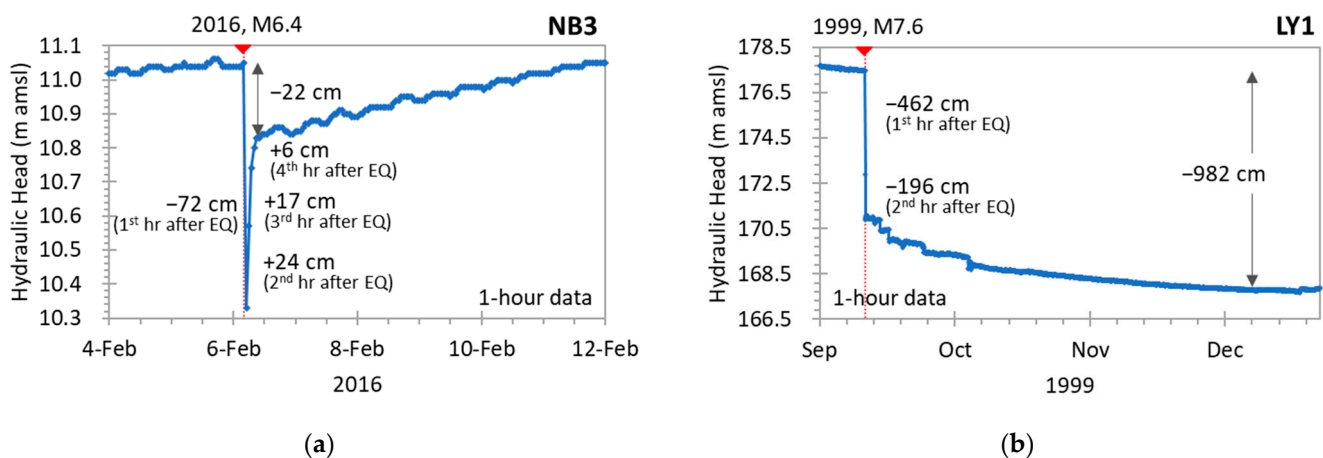


Figure 6. Abnormal post-seismic changes in groundwater level: (a) post-seismic changes after a coseismic fall of 72 cm in well NB3 due to the 2016 M6.4 earthquake; (b) post-seismic changes after a coseismic fall of 658 cm in well LY1 due to the 1999 M7.6 earthquake.

3.2. Spatial Distribution of Coseismic Changes

The water level data recorded at multiple-well monitoring stations provide the opportunity to enhance our understanding concerning the variation of coseismic groundwater level changes with increasing depth. As monitoring well stations are evenly distributed in the plains, basins, and valleys, it is possible to figure out the regional distribution pattern of coseismic changes in these areas.

3.2.1. Vertical Distribution

The magnitude of sustained coseismic change in groundwater level usually vary with depth at a multiple-well station. For instance, the hourly data at the station LG during the 1999 M7.6 earthquake indicated that the magnitude of coseismic rise fluctuated in wells of different depths (Figure 7a). Wells LG1, LG2, and LG3 were screened at depths of 25–34 m, 108–120 m, and 180–198 m, respectively. The largest coseismic rise of 522 cm was recorded at LG2 tapping a gravel aquifer at the intermediate depth. The smallest rise of 62 cm was recorded at LG1 tapping a shallow sand aquifer. A rise of 347 cm was recorded at LG3 tapping a deep sand aquifer. The magnitude of sustained coseismic change usually follows a particular pattern, i.e., an increase or decrease with increasing depth and

depends on the type, thickness, and grain size of the aquifers as well. Apparently, the magnitudes of sustained coseismic rises in LG1, LG2, and LG3 do not follow a particular pattern with increasing depth, but they are likely to be associated with the elastic properties and thickness of aquifer.

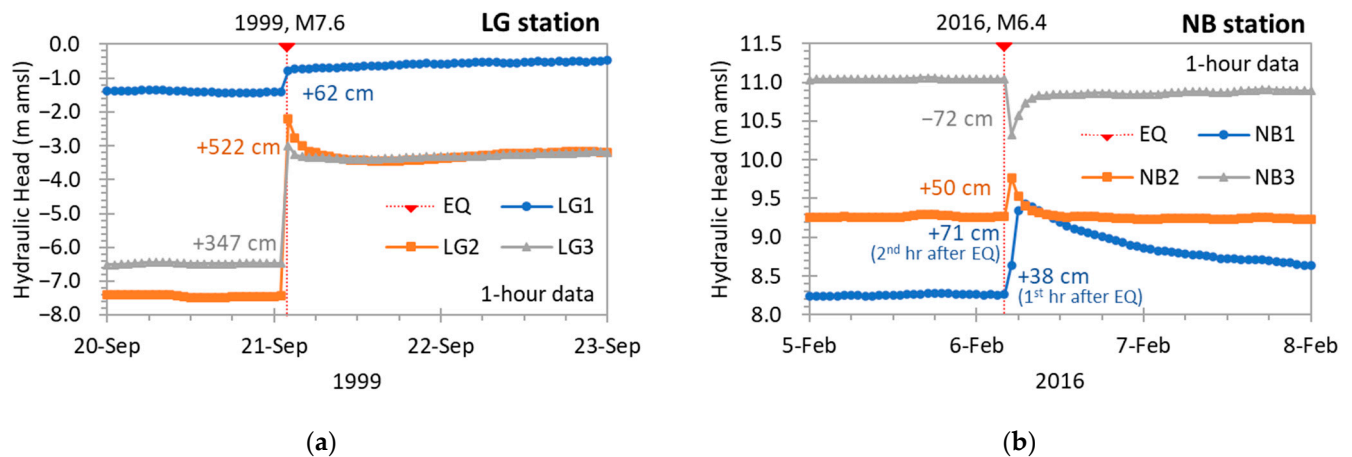


Figure 7. Vertical distribution of coseismic changes in the multiple-well stations: (a) the magnitude of coseismic rises changed with depths at the LG station during the 1999 M7.6 earthquake; (b) two coseismic rises and one fall were recorded in wells of different depths at the NB station during the 2016 M6.4 earthquake.

However, the amount of coseismic change might relate to the aquifer's properties. A previous study indicated that a relatively large coseismic rise at a station typically occurs in a gravel aquifer, rather than in a sand aquifer [34], and this is the same as what was observed in this study. This phenomenon is obviously associated with the physical properties of the aquifer and is consistent with the concept of poroelastic theory [23].

At some multiple-well stations, the polarity of coseismic changes of groundwater level varies from a fall to a rise in wells of different depths. Figure 7b shows coseismic changes at station NB during the 2016 M6.4 earthquake. A coseismic fall was recorded in the shallow well NB1, while two coseismic rises were recorded in the other two deeper wells NB2 and NB3. The vertical distribution of coseismic changes at station NB implied that crustal deformation due to earthquakes is possible to vary from an extension to a compression with increasing depth.

The variation in the polarity of sustained changes with depth reveals the complexity of crustal deformation during earthquakes. It is noted that such a phenomenon has often been observed at stations located in the transition between the compression and the extension zones as well as between hills and plains.

Two consecutive M7.1 and M6.9 earthquakes occurred offshore of the southern tip of Taiwan on 26 December 2006 [38]. The focal mechanism solutions suggest normal faulting and strike-slip faulting for the first and second shocks, respectively [38]. From the 1 Hz data recorded at well TS3 during the earthquake, the doublet clearly shows two oscillatory and sustained coseismic changes [39]. Figure 8a shows the spatial distribution of coseismic changes at monitoring stations in the southern plain of Taiwan during the earthquake doublet. Coseismic rises were recorded in wells at 23 stations, whereas falls were recorded at eight stations. At the other eight stations, coseismic rises and falls were recorded in wells of different depths.

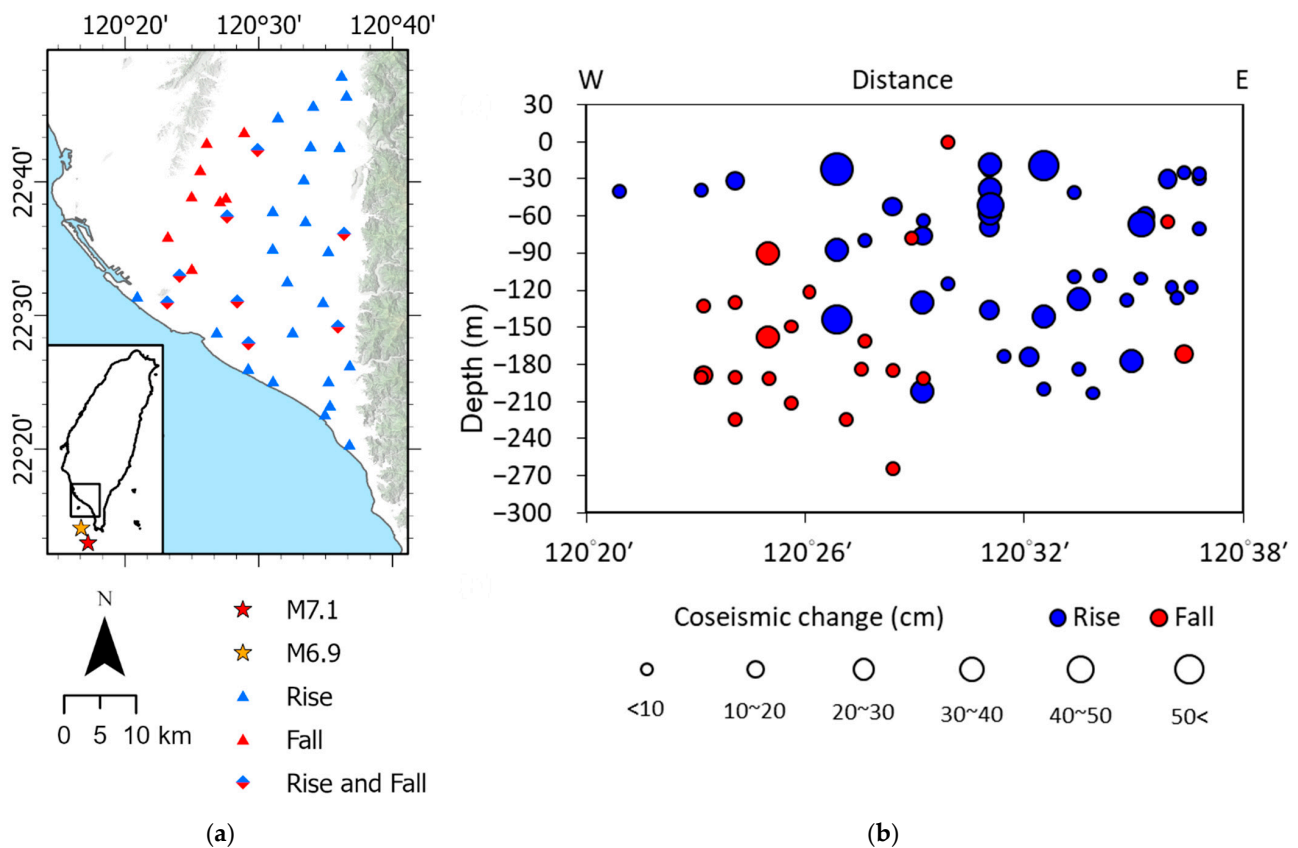


Figure 8. (a) Regional distribution of coseismic groundwater-level changes induced by the 2006 M7.1 and M6.9 earthquake doublet in the southern plain of Taiwan; (b) vertical distribution of the coseismic changes along the east–west profile.

Generally, groundwater-level falls prevailed on the west side of the southern plain, whereas rises dominated on the east side. Moreover, on the east–west profile, as shown in Figure 8b, most coseismic rises were recorded in shallow wells, while most falls were in deep wells. Such a profile revealed a distinct distribution pattern of coseismic strain in the subsurface of the southern plain in Taiwan. While crustal compression prevailed in the shallow depths, crustal extension was likely to dominate in the deep subsurface during the earthquake.

As the polarity of coseismic changes may vary with depths, subsurface deformation due to earthquakes is possibly different from surface deformation. It is envisioned that coseismic changes in groundwater level may provide information complementary to the GPS-based monitoring of surface deformation to enhance our understanding of crustal deformation in the subsurface.

3.2.2. Regional Distribution

Coseismic changes during the following three large land earthquakes in Taiwan are presented to demonstrate the complexity of regional subsurface deformation.

- 1999 M7.6 earthquake

The 1999 M7.6 earthquake occurred in central Taiwan on 21 September. The focal depth was about 8 km [40], and the focal mechanism is a thrust type with a strike of 5°, a dip of 34°, and a rake of 65° [41,42]. Widespread surface rupture resulted from thrusting along the Chelungpu fault extended approximately 100 km in the north–south direction [43]. A field investigation and GPS survey indicated lateral displacement up to 10.1 m and vertical displacement up to 8 m in the hanging wall of the fault [44]. Coseismic changes in groundwater level, ranging from −11.09 to +7.42 m, were recorded by 157 wells at

64 stations in the footwall [37]. However, no monitoring wells were installed in the hanging wall of the fault.

Figure 9 illustrates the regional distribution of coseismic changes of groundwater level in the footwall of the ruptured seismogenic fault and the corresponding geological cross-section. Based on the geological cross-section, the occurrence of an earthquake was directly generated by the Chelungpu fault and induced the coseismic groundwater level changes. It is noted that coseismic falls prevailed in the belt adjacent to the fault and the magnitude of coseismic falls increased toward the fault. Such a distribution that suggests crustal extension occurred near the ruptured fault during the earthquake and increased the permeability of aquifers. Beyond the extension belt, nearly all of them were coseismic rises, suggesting the dominance of crustal compression in the footwall during the earthquake. At a few stations in the transition between the extension and the compression zones, coseismic rises and falls were recorded in wells at different depths.

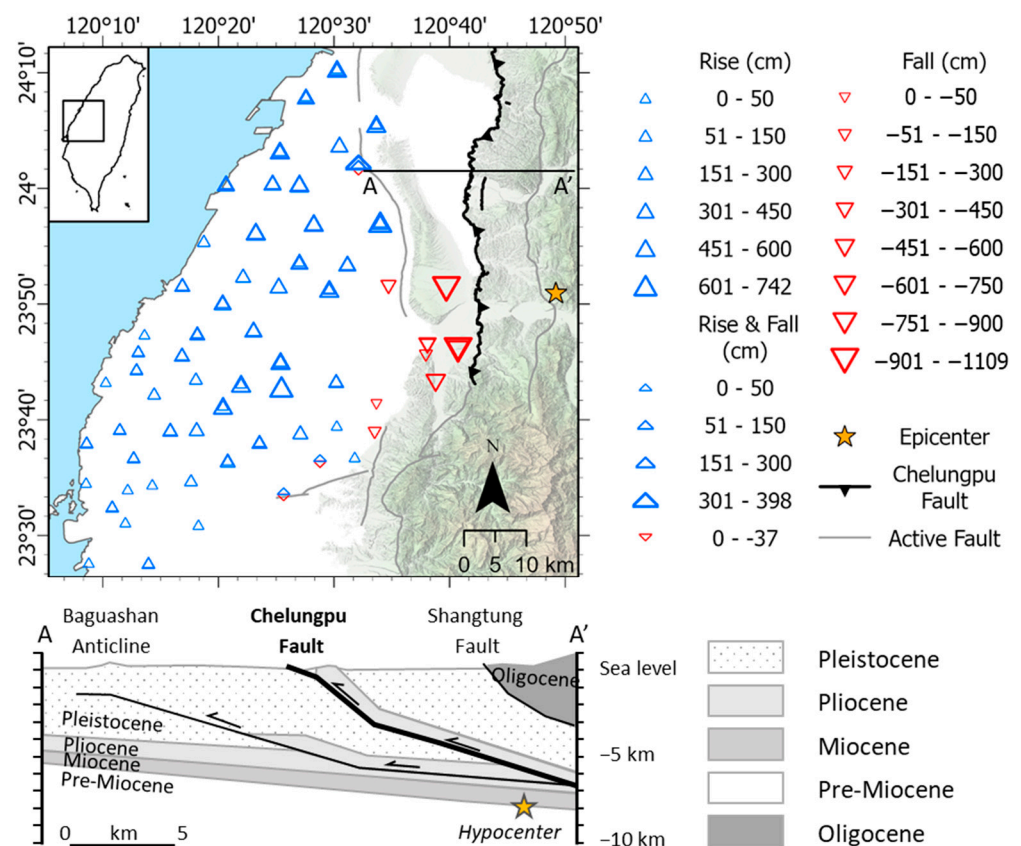


Figure 9. Distribution of coseismic groundwater level changes in the vicinity of a ruptured fault due to the 1999 M7.6 earthquake and the corresponding simplified geological cross-section of AA' (adopted from [45,46]).

- 2010 M6.3 earthquake

The 2010 M6.3 earthquake occurred in the mountainous area of southern Taiwan on 4 March. The focal mechanism indicates that the earthquake was the result of thrust faulting, with two nodal planes of NE–SW striking, NW dipping; and NW–SE striking, NE dipping faults, respectively [47]. GPS survey indicated that the maximum horizontal coseismic displacement was 3.9 cm, located 15 to 16 km W to WNW of the epicenter, and the deformation decreased to the northwest [48].

Most coseismic changes were recorded in the southwestern plain and the southern plain on the west side of Taiwan (Figure 10). Among 372 wells installed in these areas, 195 wells recorded coseismic groundwater level changes, ranging from –50 to +192 cm.

These changes included 173 rises and 22 falls. Therefore, coseismic changes were recorded at 52% of these wells, and 88% of these changes were rises. Large coseismic falls were recorded primarily in the middle of the southwest plain, rather than the vicinity of the epicenter.

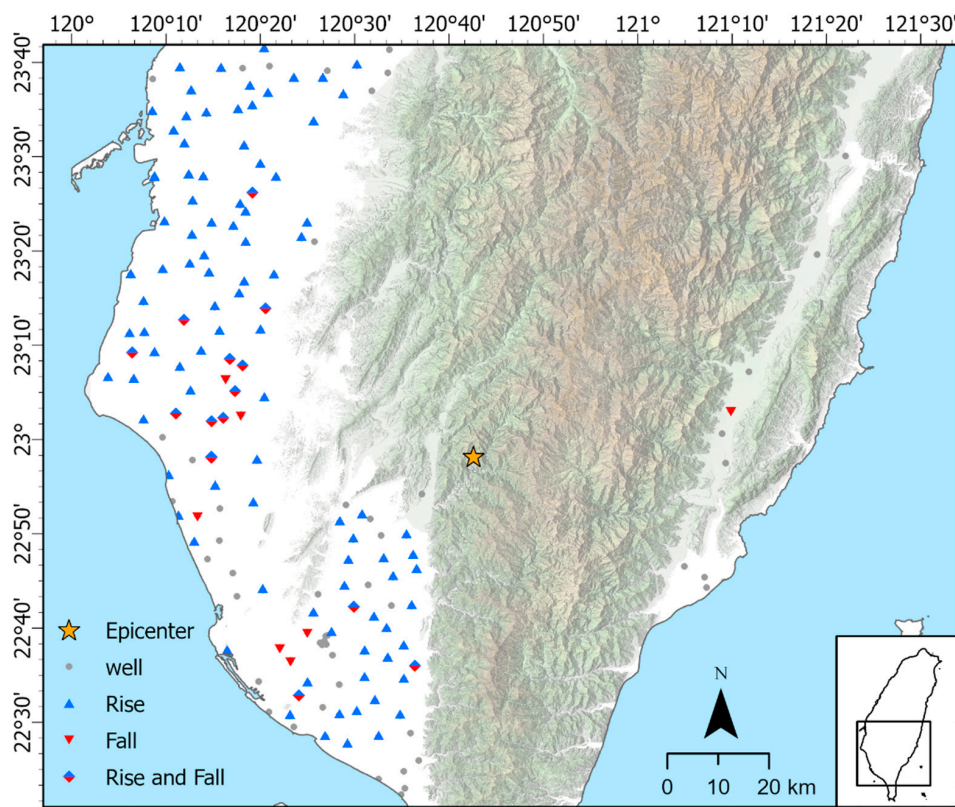


Figure 10. Distribution of coseismic groundwater level changes in southern Taiwan due to the 2010 M6.3 earthquake.

On the east side of Taiwan, among 22 monitoring wells installed in the unconsolidated deposits of the longitudinal valley, only one small coseismic fall was recorded. In other words, only 4.5% of these wells recorded coseismic changes, far below that on the west side of Taiwan. The longitudinal valley lies right on the convergent boundary between the Eurasian plate and the Philippine Sea plate. Intensive crustal deformation is expected to occur along the convergent boundary. However, the groundwater level data in the longitudinal valley consistently show a weak coseismic response to large earthquakes, except those that have occurred inside the valley. Such a phenomenon is possibly caused by the concentration of stress change on the mountains adjacent to the valley, instead of deposits in the valley during earthquakes.

- 2016 M6.4 earthquake

The 2016 M6.4 earthquake occurred on 6 February in southern Taiwan due to oblique thrust faulting at a depth of approximately 23 km [49]. The coseismic changes in groundwater level were recorded in 300 wells at 172 stations. Similar to the case of 2010 M6.3 earthquake, coseismic rises were recorded in more than 80% of these wells. Since Taiwan Island was formed by a collision between the Eurasian Plate and the Philippine Sea Plate, widespread coseismic rises are expected to occur in the area during earthquakes.

The regional distribution of coseismic changes in groundwater level triggered by the 2016 M6.4 earthquake is shown in Figure 11a. The distribution did not show any clear pattern of crustal compression and extension. It is noted, however, that most coseismic falls were recorded in the southwestern plain. Such a phenomenon has been observed during most large earthquakes, possibly associated with the local tectonic setting.

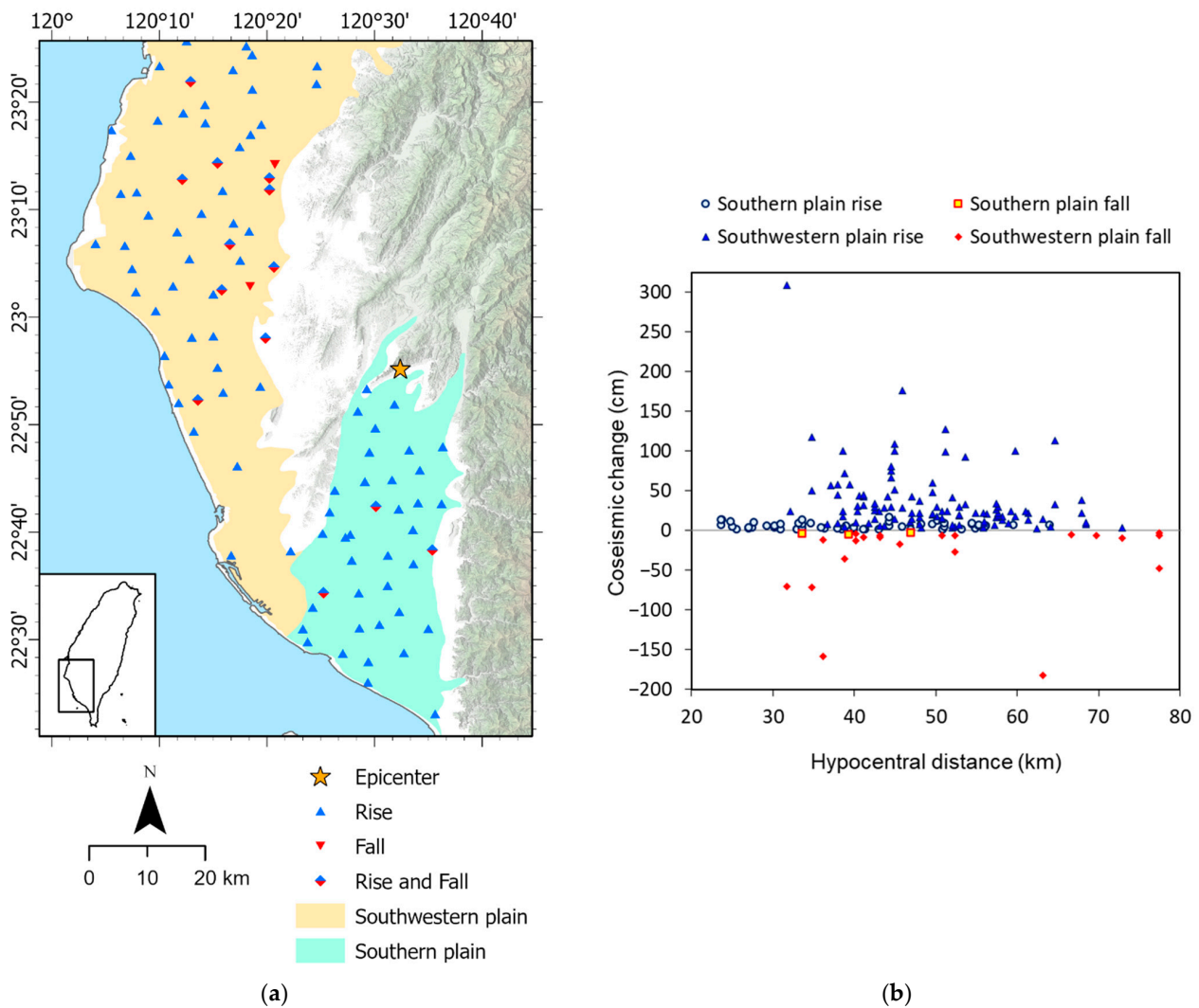


Figure 11. (a) Regional distribution of coseismic groundwater level changes in southwestern Taiwan due to the 2016 M6.4 earthquake; (b) magnitude of coseismic rises and falls versus hypocentral distance in the southern plain and southwestern plain.

The earthquake epicenter was located near the northern tip of the southern plain. However, only small to moderate coseismic changes, ranging from -5 to $+17$ cm, were recorded in the southern plain. On the other hand, in the southwestern plain, coseismic changes ranging from -183 to $+309$ cm were recorded. More than 20% of these changes were greater than 50 cm (Figure 11b). Such large changes might be caused by the occurrence of a triggered slip on a shallower duplex thrust structure in the southwestern plain shortly after the mainshock [50].

4. Discussion

4.1. Impacts of Coseismic Changes

Sustained changes in groundwater level due to large earthquakes may have profound impacts on the post-seismic hydrological processes of groundwater and surface water systems. A large coseismic fall in groundwater level is anticipated to drive groundwater flow from surrounding formations after an earthquake. The possible consequence is a modified subsurface flow pattern and a gradual decrease in pore pressure in the shallow formations over a period of months to years. Conversely, a large coseismic rise may cause a gradual increase in pore pressure in the shallow formations. Such a post-seismic

change in the subsurface is likely to alter the discharge of stream flow or spring flow after large earthquakes [17].

Moreover, a large coseismic fall may increase the effective stress of the aquifer and its confining formations, triggering land subsidence due to consolidation. In addition, engineering facilities in the deep subsurface, such as tunnels, mines, or geological repositories, are likely to be influenced by the seepage resulting from a large coseismic rise in addition to ruptures.

4.2. Sustained Changes Caused by Distant Earthquakes

During the 2008 M8.1 Wenchuan earthquake, sustained changes were recorded at 80 wells in Taiwan, where the epicentral distance is approximately 1900 km. On the other hand, no changes were recorded during the 2011 M9.0 Tohoku earthquake that occurred approximately 2600 km away from Taiwan.

The different response of the groundwater level to the distant earthquakes is possibly associated with plate tectonics. The 2011 M9.0 Tohoku earthquake occurred near the subduction zone of the Pacific plate beneath the Okhotsk plate along the Japan Trench, but the island of Taiwan is located at neither the Pacific plate nor the Okhotsk plate. Apparently, crustal deformation due to the 2011 earthquake cannot extend to the place of different plate. On the other hand, the 2008 M8.1 Wenchuan earthquake resulted from the convergence of the Indian Plate and the Eurasian Plate. The earthquake epicenter is located in the middle of the Eurasian plate, while Taiwan is located at the eastern boundary of the Eurasian plate. The widespread sustained changes in groundwater level in Taiwan suggest that it is possible for crustal deformation due to a large earthquake in the middle of a plate to propagate to the border of the same plate.

4.3. Rapid Recovery Due to Strain Relief

The rapid rise in groundwater level in 4 h right after a coseismic fall of 72 cm in well NB3 during the 2016 M6.4 earthquake, as shown in Figure 6a, is worthy of attention. Such a rapid recovery after a coseismic change has rarely been observed. The normal recovery process at NB3 (Figure 5b) implied that the rapid rise was not caused by groundwater inflow driven by the coseismic fall. Well NB3 is not installed in the unconfined or semi-confined aquifer, and no injection activities in the vicinity of the well were found. Therefore, hydrological process could not play a major role in the rapid recovery.

Based on the poroelastic theory, the rise in pore pressure can be generated by the change in stress–strain, in addition to groundwater flow. Therefore, the rapid recovery in the groundwater level after the coseismic change was possibly associated with post-seismic relaxation of crustal deformation [51]. In the case of well NB3, rapid relief of the extension strain might have occurred immediately after the 2016 M6.4 earthquake. However, further studies and alternative monitoring approaches are needed to investigate and understand the process of strain relief.

4.4. Factors Controlling Spatial Distribution

For the local earthquakes used in this study, coseismic rises prevail in most areas, suggesting that crustal compression caused by plate convergence plays a major role on the island of Taiwan during earthquakes. However, for large, distant earthquakes, no particularly spatial patterns were observed.

Our studies associated with the spatial distributions of coseismic changes revealed complex vertical and regional variations of crustal deformation due to fault slip. Irregular distribution pattern of coseismic rises and falls have commonly been observed, possibly associated with the local tectonic setting, aquifer characteristics, topography, and geological conditions in addition to the focal mechanism. It is difficult to establish a comprehensive model for the interpretation of the distribution of the polarity and the magnitude of recorded sustained changes. More information on coseismic changes and theoretical studies of mechanisms are desirable for a better understanding of the vertical and regional

distributions of sustained changes in groundwater level caused by crustal deformation during large earthquakes.

4.5. High-Frequency Monitoring

Recently developed, high-frequency automated recording techniques have significantly improved water level monitoring for earthquake activities. High-frequency monitoring has the advantage of recording the detailed process of water level changes. The recorded water level data do not need to be corrected for the effects of rainfall, earth tide, and barometric pressure. Any missing data due to clock error can be easily detected and corrected. At present, the maintenance of high-frequency monitoring systems is time-consuming and cost-intensive. However, the advancement and improvement of digital technology are expected to ease the burden in the near future.

5. Conclusions

The following conclusions and recommendations can be drawn from our study on the temporal variations and spatial distributions of sustained coseismic changes in groundwater level:

1. Coseismic sustained changes usually recover slowly after earthquakes. Occasionally, abnormal post-seismic changes in groundwater level were observed, possibly associated with cross-formation flow, fracturing, or strain relief.
2. Widespread sustained changes in Taiwan triggered by the 2008 M8.1 earthquake suggested that crustal deformation due to fault rupture in the middle of a tectonic plate could extend a long distance to the plate boundary.
3. The polarity and magnitude of sustained changes in groundwater level may vary with depths, providing information on subsurface deformation supplementary to the monitoring of surface deformation.
4. Water level data recorded during the 1999 M7.6 earthquake indicated that coseismic falls prevailed in the area adjacent to the seismogenic fault, implying the dominance of crustal extension near the ruptured thrust fault.
5. In the vicinity of a convergent plate boundary, coseismic rises in groundwater level often dominate due to crustal compression caused by thrust faulting.

High-frequency monitoring is recommended for studies of groundwater level changes induced by earthquakes. Moreover, integration of groundwater monitoring with GPS monitoring may provide more comprehensive information for crustal deformation during earthquakes.

Author Contributions: Conceptualization, C.-Y.L., Y.C. and Y.-C.C.; methodology, C.-Y.L., Y.C., P.-Y.C. and T.-P.L.; validation, Y.C. and Y.-C.C.; formal analysis, C.-Y.L.; investigation, Y.C. and Y.-C.C.; resources, Y.C., P.-Y.C. and T.-P.L.; data curation, C.-Y.L., Y.C. and Y.-C.C.; writing—original draft preparation, C.-Y.L., Y.C. and Y.-C.C.; writing—review and editing, Y.C. and Y.-C.C.; visualization, C.-Y.L.; supervision, Y.C. and Y.-C.C.; project administration, Y.C.; funding acquisition, Y.C. All authors have read and agreed to the published version of the manuscript.

Funding: This research was funded by Water Resources Agency, Ministry of Economic Affairs of Taiwan, grant number MOEAWRA0960016; National Science and Technology Council of Taiwan, grant numbers NSC100-2116-M002-017, NSC 102-2116-M-002-013, and MOST105-2116-M002-023.

Data Availability Statement: Not applicable.

Acknowledgments: We would like to acknowledge Yi-Hsuan Chiang for the supporting data analysis and Chien-Chung Ke for supporting the work.

Conflicts of Interest: The authors declare no conflict of interest. The funders had no role in the design of the study; in the collection, analysis, or interpretation of data; in the writing of the manuscript; or in the decision to publish the results.

References

1. Waller, R. Effects of the March 1964 Alaska earthquake on the hydrology of the Anchorage area, Alaska. In *The Alaska Earthquake, March 27, 1964: Effects on the Hydrologic Regimen (Professional Paper 544)*, 1st ed.; U.S. Government Printing Office: Washington, DC, USA, 1966; Chapter B; pp. B1–B18.
2. Grecksch, G.; Roth, F.; Kumpel, H.J. Co-seismic well-level changes due to the 1992 Roermond earthquake compared to static deformation of half-space solutions. *Geophys. J. Int.* **1999**, *138*, 470–478. [[CrossRef](#)]
3. Wang, C.Y.; Manga, M. *Earthquakes and Water*, 1st ed.; Springer: Berlin/Heidelberg, Germany, 2010; pp. 67–95.
4. Kinoshita, C.; Kano, Y.; Ito, H. Shallow crustal permeability enhancement in central Japan due to the 2011 Tohoku earthquake. *Geophys. Res. Lett.* **2015**, *42*, 773–780. [[CrossRef](#)]
5. Wakita, H. Water wells as possible indicators of tectonic strain. *Science* **1975**, *189*, 553–555. [[CrossRef](#)] [[PubMed](#)]
6. Roeloffs, E.A.; Burford, S.S.; Riley, F.S.; Records, A.W. Hydrologic effects on water level changes associated with episodic fault creep near Parkfield, California. *J. Geophys. Res.* **1989**, *94*, 12387–12402. [[CrossRef](#)]
7. Montgomery, D.R.; Manga, M. Streamflow and water well responses to earthquakes. *Science* **2003**, *300*, 2047–2049. [[CrossRef](#)]
8. Cooper, H.H.; Bredehoeft, J.D.; Papadopoulos, I.S.; Bennett, R.R. The response of well-aquifer systems to seismic waves. *J. Geophys. Res.* **1965**, *70*, 3915–3926. [[CrossRef](#)]
9. Ohno, M.; Wakita, H.; Kanjo, K. A water well sensitive to seismic waves. *Geophys. Res. Lett.* **1997**, *24*, 691–694. [[CrossRef](#)]
10. Kitagawa, Y.; Itaba, S.; Matsumoto, N.; Koizumi, N. Frequency characteristics of the response of water pressure in a closed well to volumetric strain in the high-frequency domain. *J. Geophys. Res.* **2011**, *116*, B08301–B08312. [[CrossRef](#)]
11. Liu, C.Y.; Chia, Y.; Chuang, P.Y.; Chiu, Y.C.; Tseng, T.L. Impacts of hydrogeological characteristics on groundwater-level changes induced by earthquakes. *Hydrogeol. J.* **2018**, *26*, 451–465. [[CrossRef](#)]
12. Hosono, T.; Yamada, C.; Shibata, T.; Tawara, Y.; Wang, C.Y.; Manga, M.; Rahman, A.T.M.S.; Shimada, J. Coseismic Groundwater Drawdown Along Crustal Ruptures During the 2016 M_w 7.0 Kumamoto Earthquake. *Water Resour. Res.* **2019**, *55*, 5891–5903. [[CrossRef](#)]
13. Lee, T.P.; Chia, Y.; Yang, H.Y.; Liu, C.Y.; Chiu, Y.C. Groundwater Level Changes in Taiwan Caused by The Wenchuan Earthquake on 12 May 2008. *Pure Appl. Geophys.* **2012**, *169*, 1947–1962. [[CrossRef](#)]
14. He, A.; Zhao, G.; Sun, Z.; Singh, R.P. Co-seismic multilayer water temperature and water level changes associated with Wenchuan and Tohoku-Oki earthquakes in the Chuan no. 03 well, China. *J. Seismol.* **2016**, *21*, 719–734. [[CrossRef](#)]
15. Liu, C.Y.; Chia, Y.; Chuang, P.Y.; Wang, C.Y.; Ge, S.; Teng, M.H. Streamflow Changes in the Vicinity of Seismogenic Fault After the 1999 Chi–Chi Earthquake. *Pure Appl. Geophys.* **2018**, *175*, 2425–2434. [[CrossRef](#)]
16. Weaver, K.C.; Cox, S.C.; Townend, J.; Rutter, H.; Hamling, I.J.; Holden, C. Seismological and Hydrogeological Controls on New Zealand-Wide Groundwater Level Changes Induced by the 2016 M_w 7.8 Kaikōura Earthquake. *Geofluids* **2019**, *2019*, 9809458. [[CrossRef](#)]
17. Manga, M.; Wang, C.Y.; Shirzaei, M. Increased stream discharge after the 3 September 2016 M_w 5.8 Pawnee, Oklahoma earthquake. *Geophys. Res. Lett.* **2016**, *43*, 11588–11594. [[CrossRef](#)]
18. Mohr, C.H.; Manga, M.; Wang, C.Y.; Korup, O. Regional changes in streamflow after a megathrust earthquake. *Earth Planet. Sci. Lett.* **2017**, *458*, 418–428. [[CrossRef](#)]
19. Wang, C.Y.; Manga, M.; Wang, C.H.; Chen, C.Y. Earthquakes and subsurface temperature changes near an active mountain front. *Geology* **2012**, *40*, 119–122. [[CrossRef](#)]
20. Miyakoshi, A.; Taniguchi, M.; Ide, K.; Kagabu, M.; Hosono, T.; Shimada, J. Identification of changes in subsurface temperature and groundwater flow after the 2016 Kumamoto earthquake using long-term well temperature–depth profiles. *J. Hydrol.* **2020**, *582*, 124530–124539. [[CrossRef](#)]
21. Igarashi, G.; Saeki, S.; Takahata, N.; Sumikawa, K.; Tasaka, S.; Sasaki, Y.; Takahashi, M.; Sano, Y. Ground-Water Radon Anomaly Before the Kobe Earthquake in Japan. *Science* **1995**, *269*, 60–61. [[CrossRef](#)]
22. Skelton, A.; Andrén, M.; Kristmannsdóttir, H.; Stockmann, G.; Mörth, C.M.; Sveinbjörnsdóttir, Á.; Jónsson, S.; Sturkell, E.; Guðrúnardóttir, H.R.; Hjartarson, H.; et al. Changes in groundwater chemistry before two consecutive earthquakes in Iceland. *Nature Geosci.* **2014**, *7*, 752–756. [[CrossRef](#)]
23. Biot, M.A. General theory of three-dimensional consolidation. *J. Appl. Phys.* **1941**, *12*, 155–164. [[CrossRef](#)]
24. Biot, M.A. Theory of Elasticity and Consolidation for a Porous Anisotropic Solid. *J. Appl. Phys.* **1955**, *26*, 182–185. [[CrossRef](#)]
25. Rice, J.R.; Cleary, M.P. Some basic stress diffusion solutions for fluid-saturated elastic porous media with compressible constituents. *Rev. Geophys. Space Phys.* **1976**, *14*, 227–241. [[CrossRef](#)]
26. Palciauskas, V.; Domenico, P. Fluid pressures in deforming porous rocks. *Water Resour. Res.* **1989**, *25*, 203–213. [[CrossRef](#)]
27. Roeloffs, E.A. Poroelastic techniques in the study of earthquake-related hydrologic phenomena. *Adv. Geophys.* **1996**, *37*, 135–195.
28. Caporali, A.; Braitenberg, C.; Massironi, M. Geodetic and hydrological aspects of the Merano earthquake of 17 July 2001. *J. Geodyn.* **2005**, *39*, 317–336. [[CrossRef](#)]
29. McCormack, K.A.; Hesse, M.A. Modeling the poroelastic response to megathrust earthquakes: A look at the 2012 M_w 7.6 Costa Rican event. *Adv. Water Resour.* **2018**, *114*, 236–248. [[CrossRef](#)]
30. Lee, J.C.; Angelier, J.; Chu, H.T.; Yu, S.B.; Hu, J.C. Plate-boundary strain partitioning along the sinistral collision suture of the Philippine and Eurasian plate: Analysis of geodetic data and geological observation in southeastern Taiwan. *Tectonics* **1998**, *17*, 859–871. [[CrossRef](#)]

31. Muir-Wood, R.; King, G.C.P. Hydrological signatures of earthquake strain. *J. Geophys. Res.* **1993**, *98*, 22035–22068. [[CrossRef](#)]
32. Wang, H.F. Effects of deviatoric stress on undrained pore pressure response to fault slip. *J. Geophys. Res.* **1997**, *102*, 17943–17950. [[CrossRef](#)]
33. Wang, C.Y.; Dreger, D.; Manga, M.; Wong, A. Streamflow increase due to rupturing of hydrothermal reservoirs: Evidence from the 2003 San Simeon, California, earthquake. *Geophys. Res. Lett.* **2004**, *31*, L10502–L10506. [[CrossRef](#)]
34. Chia, Y.; Chiu, J.J.; Chiang, Y.H.; Lee, T.P.; Wu, Y.M.; Horng, M.J. Implications of coseismic groundwater level changes observed at multiple-well monitoring stations. *Geophys. J. Int.* **2008**, *172*, 293–301. [[CrossRef](#)]
35. Cox, S.C.; Rutter, H.K.; Sims, A.; Manga, M.; Weir, J.J.; Ezzy, T.; White, P.A.; Horton, T.W.; Scott, D. Hydrological effects of the M W 7.1 Darfield (Canterbury) earthquake, 4 September 2010, New Zealand. *N. Z. J. Geol. Geophys.* **2012**, *55*, 231–247. [[CrossRef](#)]
36. King, C.Y.; Azuma, S.; Igarashi, G.; Ohno, M.; Saito, H.; Wakita, H. Earthquake related water-level changes at 16 closely clustered wells in Tono, Central Japan. *J. Geophys. Res.* **1999**, *104*, 13073–13082. [[CrossRef](#)]
37. Chia, Y.; Wang, Y.S.; Chiu, J.J.; Liu, C.W. Changes of groundwater level due to the 1999 Chi-Chi earthquake in the Choshui River alluvial fan in Taiwan. *Bull. Seism. Soc. Am.* **2001**, *91*, 1062–1068. [[CrossRef](#)]
38. USGS, Earthquake Hazards Program. Available online: <http://earthquake.usgs.gov/earthquakes/eventpage/usp000f114#executive> (accessed on 29 October 2022).
39. Chia, Y.; Chiu, J.; Chung, P.Y.; Chang, Y.L.; Lai, W.C.; Kuan, Y.C. Spatial Distribution of Groundwater Level Changes Induced by the 2006 Hengchun Earthquake Doublet. *Terr. Atmos. Ocean. Sci.* **2009**, *20*, 315–324. [[CrossRef](#)]
40. Shin, T.C.; Kuo, K.W.; Lee, W.H.K.; Teng, T.L.; Tsai, Y.B. A Preliminary Report on the 1999 Chi-Chi (Taiwan) Earthquake. *Seism. Res. Lett.* **2000**, *71*, 24–30. [[CrossRef](#)]
41. Kao, H.; Chen, W.P. The Chi-Chi Earthquake Sequence: Active, Out-of-Sequence Thrust Faulting in Taiwan. *Science* **2000**, *288*, 2346–2349. [[CrossRef](#)]
42. Chang, C.H.; Wu, Y.M.; Shin, T.C.; Wang, C.Y. Relocation of the 1999 Chi-Chi Earthquake in Taiwan. *Terr. Atmos. Ocean. Sci.* **2000**, *11*, 581–590. [[CrossRef](#)]
43. Angelier, J.; Lee, J.C.; Chu, H.T.; Hu, J.C. Reconstruction of fault slip of the September 21st, 1999, Taiwan earthquake in the asphalted surface of a car park, and co-seismic slip partitioning. *J. Struct. Geol.* **2003**, *25*, 345–350. [[CrossRef](#)]
44. Central Geological Survey of Taiwan. Groundwater observation well network in Taiwan area: Hydrogeologic investigation in the Choshui River alluvial fan. *CGS Rep.* **1999**, 008414880022. (In Chinese)
45. Johnson, K.M.; Segall, P. Imaging the ramp–de’collement geometry of the Chelungpu fault using coseismic GPS displacements from the 1999 Chi-Chi, Taiwan earthquake. *Tectonophysics* **2004**, *378*, 123–139. [[CrossRef](#)]
46. Lee, J.C.; Chen, Y.G.; Sieh, K.; Mueller, K.; Chen, W.S.; Chu, H.T.; Chan, Y.C.; Rubin, C.; Yeats, R. A Vertical Exposure of the 1999 Surface Rupture of the Chelungpu Fault at Wufeng, Western Taiwan: Structural and Paleoseismic Implications for an Active Thrust Fault. *BSSA* **2004**, *91*, 914–929. [[CrossRef](#)]
47. Huang, M.H.; Dreger, D.; Bürgmann, R.; Yoo, S.H.; Hashimoto, M. Joint inversion of seismic and geodetic data for the source of the 2010 March 4, Mw 6.3 Jia-Shian, SW Taiwan, earthquake. *Geophys. J. Int.* **2013**, *193*, 1608–1626. [[CrossRef](#)]
48. Central Geological Survey of Taiwan. 20100304 earthquake geological survey report. *CGS Rep.* **2010**. (In Chinese)
49. USGS, Earthquake Hazards Program. Available online: <https://earthquake.usgs.gov/earthquakes/eventpage/us20004y6h/executive> (accessed on 29 October 2022).
50. Huang, M.H.; Tung, H.; Fielding, E.J.; Huang, H.H.; Liang, C.; Huang, C.; Hu, J.C. Multiple fault slip triggered above the 2016 Mw 6.4 MeiNong earthquake in Taiwan. *Geophys. Res. Lett.* **2016**, *43*, 7459–7467. [[CrossRef](#)]
51. Liu, K.; Geng, J.; Wen, Y.; Ortega-Culaciati, F.; Comte, D. Very Early Postseismic Deformation Following the 2015 Mw 8.3 Illapel Earthquake, Chile Revealed From Kinematic GPS. *Geophys. Res. Lett.* **2022**, *29*, e2022GL098526. [[CrossRef](#)]

Disclaimer/Publisher’s Note: The statements, opinions and data contained in all publications are solely those of the individual author(s) and contributor(s) and not of MDPI and/or the editor(s). MDPI and/or the editor(s) disclaim responsibility for any injury to people or property resulting from any ideas, methods, instructions or products referred to in the content.